25th ABCM International Congress of Mechanical Engineering
October20-25, 2019, Uberlândia, MG, Brazil

COB-2019-2154
COMPARATIVE STUDY OF RESIDUAL STRESSES IN GRINDING OF P91 STEEL BY X-RAY DIFFRACTION AND MAGNETIC BARKHAUSEN NOISE TECHNIQUE

Maria Cindra Fonseca
Gabriele Magalhães
Matheus Thomaz Muntzberg
Leosdan F. Noris
Bernardo Moniz
Bruna Machado
UFF – Universidade Federal Fluminense – Departamento de Engenharia Mecânica/ PGMEC, Rua Passo da Pátria, 156, Bloco D, Sala 302, CEP 24210-240, São Domingos, Niterói – RJ
mcindra@vm.uff.br
gabrielemp@id.uff.br
matheusmuntzberg@id.uff.br
leosdanfnoris@gmail.com
bernardomoniz@id.uff.br
bruna.smachadoc@gmail.com

Abstract. *The grinding process has critical importance for metal-mechanic industry, once it is a finishing machining process. The Cr-Mo steel ASTM P91 is a distinguished material used in the energy production industry, especially in power plants. Although there are many studies about the mechanical behavior of this steel, their application in machining processes is still poorly studied. Since residual stresses are intrinsic to all manufacturing processes, it is important to know the nature of these stresses, in order to avoid a premature and unexpected fracture, mainly if they are tensile stresses, which are deleterious to the fatigue life of the component. On another hand, it is well established that compressive residual stresses increase the fatigue life and the corrosion resistance of the material. Therefore, finding alternative measurement techniques that offer possibilities in quantification and qualification of residual stresses is crucial especially in field applications. In the present work, analysis of residual stresses in P91 steel samples were carried out with two different techniques: X-ray diffraction and magnetic Barkhausen noise. The results show that magnetic Barkhausen noise (MBN) values are coherent with the residual stresses measured by X-ray diffraction.*

Keywords: *P91 steel, residual stresses, X-ray diffraction, magnetic Barkhausen noise technique*

1. INTRODUCTION

Modified 9Cr-1Mo ferritic steel is widely used for steam generator applications in fossil-fuel thermal and nuclear energy industries. P91 steel is a high quality material used in power plants, due to its excellent properties: good corrosion and creep resistances at high temperatures (Choudhary and Chistopher, 2019; Pandey et al., 2018).

Machining is a family of shaping operations in which the excess material is removed by a cutting tool with the purpose of altering the geometry, properties or appearance of a raw material, resulting in parts of a product. Among the conventional machining operations are turning, milling, drilling and grinding (Groover, 2014). Grinding is usually the last machining operation applied to a component, hence the knowledge of residual stresses after grinding has a great influence on the service life of the workpiece.

Residual stresses are self-balanced and they are present in all manufactured components. They are a product of the metallurgic and the mechanical history from each portion of the component or the component as a whole, during machining processes (Cindra Fonseca et al., 2007).

These stresses influence the mechanical properties and particularly the fatigue resistance of the material, so the knowledge of their nature - tensile or compressive - and their magnitude is very important. In some cases, premature failure could be a result of a tensile stress state combined with work stresses, even though in the plastic behavior field. It is well known that tensile residual stresses are deleterious and reduce the fatigue life, increasing stress corrosion tendency. On the other hand, compressive stresses are beneficial, suppressing crack nucleation and propagation (Li et al., 2018).

There are many techniques for residual stresses measurement, such as X-ray and neutron diffraction, hole-drilling, ultrasound, magnetic Barkhausen noise, etc. (Qimeng Zhu et al., 2017). In this context, the current work analyses residual stresses in P91 steel samples using X-ray diffraction and magnetic Barkhausen noise technique (MBN).

The first technique is well established and very efficient in determining the residual stress state, once it allows qualifying and quantifying these stresses in magnitude and directions for each point of the component. Its principles were studied over fifty years ago and are based on two theories: X-ray diffraction theory and elasticity theory. The second technique has been studied for this application and it is interesting because the mechanical stresses and microstructural discontinuities apply a movement in the magnetic domain walls of ferromagnetic materials, during the magnetization process, being a non-destructive process and showing huge potential in field applications (Sorsa et al., 2018).

Statistical tests can be divided in groups of dependent and independent variables, according to the normality assumptions of residuals, homogeneity of variances, effects of variation factors and independence of the errors. The fulfillment of these requirements conditions the first choice of the test to be performed, since the parametric statistic, whose tests are in general more powerful than the tests of nonparametric statistic, can be used (Wang et al., 2017).

2. MATERIALS AND METHODS

In the present work, 6 samples of P91 steel were studied, with dimensions of 10 x 17 x 62 mm. The chemical composition and the mechanical properties of the material are shown in Tables 1 and 2, respectively. The samples were grinded, with the parameters selected (constant cutting speed ─ V_c= 30 m/s, two crossfeeds: V_f= 16 m/min and 25 m/min, and cut depths - a_p of 0.050 and 0.100 mm) in order to obtain different residual stresses levels. Samples 3 and 4 were submitted to stress relief heat treatment, in order to result in reference samples, which are considered free of residual stresses.

Table 1. P91 steel chemical composition (% in weight).

C	Si	Mn	P	S	Cr	Ni	Cu
0,108	0.33	0.53	0.013	0.002	8.560	0.300	0.190
Mo	V	N	Al	Nb	Ti	As	Sn
0,870	0.221	0.053	0.012	0.067	0.003	0.006	0.150

Table 2. Mechanical properties of ASTM P91 steel.

σ_{Le} (MPa)	σ_{Lr}(MPa)	Elongation (%)
638	724	20

For grinding operation, an aluminum oxide (Al_2O_3) grinding wheel with d_{ext}205 x d_{hole}31.8 mm x 13.5 mm wide was used, showed in Figure 1. During the operation, Hydria EP cutting fluid was applied and the application method was the abundant jet, with a constant flow rate of 6 L/min. It is noteworthy that the grinding wheel was dressed every three grinding operations, with a diamond tip, in order to minimize the influence of tool wear.

Figure 1. Grinding operation. (1) Grinding Wheel; (2) Sample.

The surface residual stress was analyzed by X-ray diffraction, using the $\sin^2\psi$ method, with CrKα (λ=2.29092 Å) radiation, diffracting the ferrite (211) plane. The residual stresses were measured using a StressRad portable analyzer (Radicon), which is shown in Fig. 2 with a collimator of Ø 1.0 mm (20 kV and 4.5 mA). All measurements were carried out in the longitudinal direction of the sample, according to Figure 3.

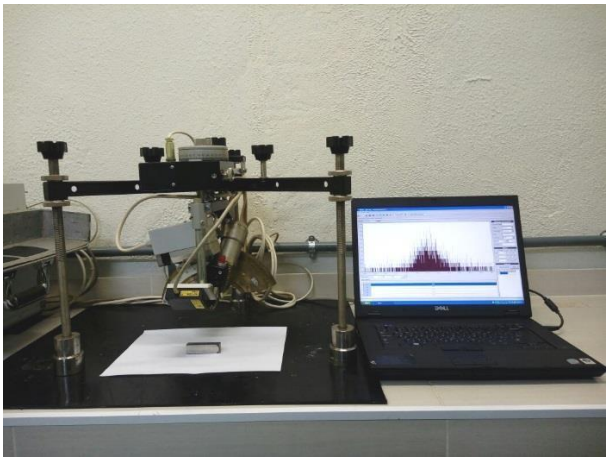

Figure 2. Stressrad stress analyzer.

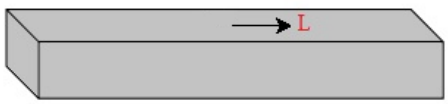

Figure 3. Point and direction of measurement of surface residual stresses on the center of the samples.

The magnetic Barkhausen noise signal was measured by BarkTech equipment, developed by LADIN Laboratory/ USP. The total control system was made by the software BarkView. The equipment setting is shown in Figure 4. The equipment is responsible for the generation and the control of the excitation current, the acquisition and the filtering of the Voltage signals generated by the RMB sensor.

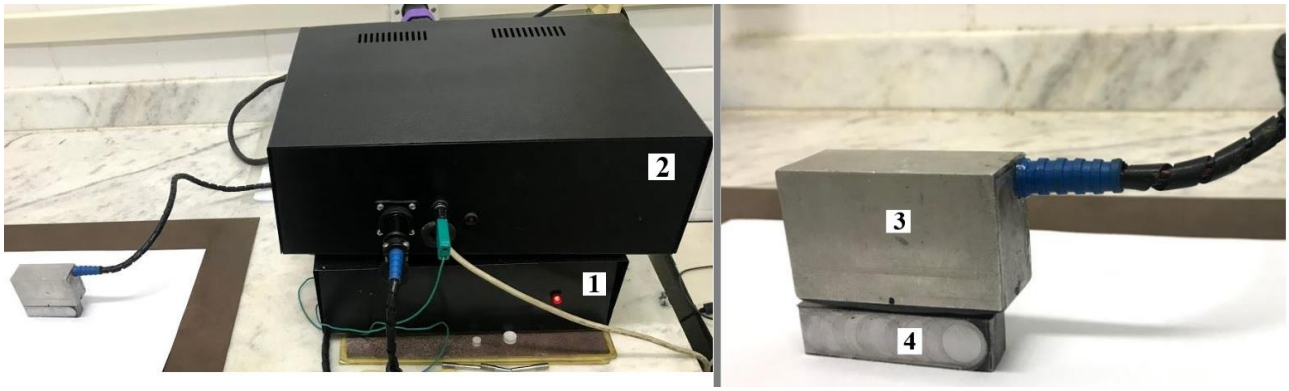

Figure 4. Measurement system by MBN: (1) Supply; (2) Signal conditioner; (3) Probe; (4) Sample.

During the measurement process, the sample-probe assembly was maintained static, according to Figure 4. The same fit parameters were used for all samples, with an excitation frequency of 40 Hz, a sampling frequency of 350 MHz and an excitation current of 3A.

3. RESULTS AND DISCUSSION

The longitudinal residual stresses results and the associated error, measured by X-ray diffraction, are shown according to the selected cutting parameters, in Table 3 and Figure 5.

Table 3. Residual stresses results.

Samples	Depth of cut ap (mm)	Crossfeed V*f* (m/min)	Residual Stresses (MPa)	
			Longitudinal	Average Residual Stress
1	0.05	16	-350 ±19	**-330**
2			-310 ±3	
3	0.1		8 ±2	**12**
4			15 ±8	
5	0.05	25	173 ± 9	**230**
6			275 ± 37	

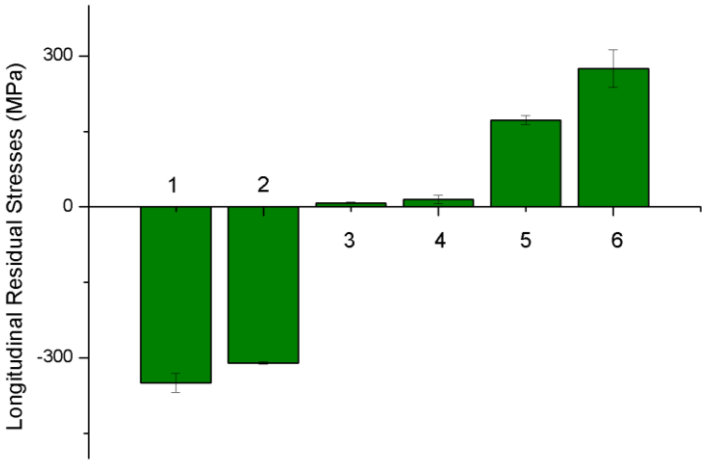

Figure 5. Longitudinal surface residual stresses.

Table 3 and Figure 4 show the longitudinal residual stresses of samples 1 to 6. For the feed rate of 16 m/min, the influence of the depth of cut on the residual stresses found in samples 1 and 2 can be verified with a cut depth of 0.05 mm, resulting in compressive residual stresses (from the order of -330 MPa). These results are coherent with those obtained by Zhou et al. (2016). These compressive residual stresses demonstrate that the cooling was done correctly, with the jet

of fluid penetrating efficiently in the cutting region, providing good lubrication, reducing friction and assuring the efficiency of the grinding wheel (Alves et al. 2009).

Samples 3 and 4 were submitted to the same grinding parameters, followed by stress relief heat treatment to be considered as references, i.e., free of residual stresses (12 MPa), enabling the correlation of the residual stresses and the noise by means of a calibration curve.

Average tensile residual stresses in longitudinal direction (230 MPa) were observed in samples 5 and 6, generated by the feed rate of 25 m/min and the depth of cut of 0.1 mm. This result that can be justified by the influence of the number of necessary passes to complete the grinding operation, once these samples received less passes than the others. This result is corroborated by Zoei et al. (2016).

In order to obtain a better evaluation of the influence of cutting parameters on the magnitude and the nature of longitudinal and transverse residual stresses, statistical tests to verify normality of residuals and homogeneity of variances were performed (Table 4). The tests were performed in *Statistica* software.

Table 4. Statistical tests.

Statistical test	Value-p
	Longitudinal Residual Stresses
Kolmogorov-Smirnov	0.6071
Shapiro-Wilk	0.8514
Levene	0.078
Hartley F-max, Cochran C, Bartlet Chi-Sqr	0.760316

Table 4 shows that the p-values were greater than 0.05, that is, the hypotheses of normality of residuals and homogeneity of variances are not rejected. For this reason, parametric statistic is used in the evaluation of the data (Table 5), and the closer to zero the p-value is, the greater the influence of the cut-off parameter evaluated.

Table 5. Parametric analysis of variance analysis for residual stresses.

Parameter	Value-p
	Longitudinal Residual Stresses
Feed rate V*f* (m/min)	0.004876
Depth of cut ap (mm)	0.04454

Table 5 shows that the feed rate is a parameter that influences longitudinal residual stresses more than the depth of cut, because the closer to zero the value of p is, the greater the influence of the parameter evaluated, consistent with Wang et al. (2017).

Table 6 presents the values of measurement of the magnetic Barkhausen noise signals in each sample.

Table 6. Magnetic Barkhausen noise (MBN).

Samples	1	2	3	4	5	6
MBN (V)	0.33	0.35	0.42	0.40	0.44	0.50
MBN average (V)	**0.34**		**0.41**		**0.47**	

Analyzing the results it is possible to observe that the amplitude signal MBN is a parameter for qualify the nature of residual stresses. In this context, tensile residual stresses set higher MBN signal levels, aligning the magnetic domains in the longitudinal stress direction, while compressive residual stresses cause lower MBN levels, aligning magnetic domains perpendicularly to the stress, which is coherent to the results obtained by Sorsa et al. (2018).

As the MBN technique does not directly provide residual stresses (MPa) results, a calibration curve was performed, (Fig. 6) to correlate the residual stresses obtained by X-ray diffraction with the MBN signals in longitudinal direction. The calibration curve was obtained by the *CurveExpert* software, using linear regression – least squares method – and the results show a determinant equation of residual stresses per MBN.

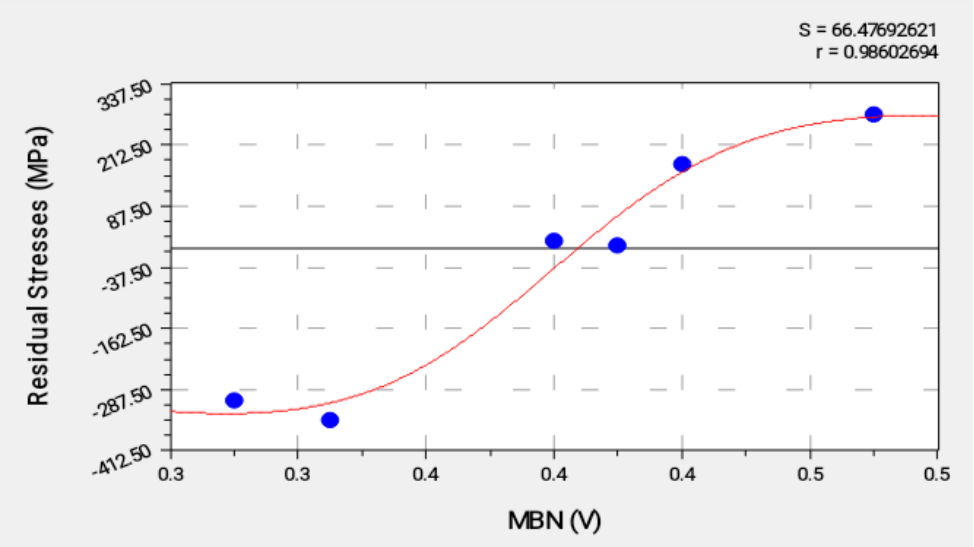

Figure 6. Calibration curve correlating X-ray diffraction and MBN values.

An equation for MBN calibration (y) was defined by the MBN signals (x) and the coefficients as shown by the Equation 1. The objective was to correlate the MBN signals, given in mV, with the residual stresses, given in MPa.

$$y = \frac{a+bx}{1+cx+dx^2} \quad (1)$$

being: a= -159.31779; b= 391.48512; c= -4.7007494; d= 5.9420432.

The values of residual stresses obtained by Eq. (1) were compared to the measurements made by X-ray diffraction, as shown in Tab. 7, to all measuring points and average residual stresses according to Fig. 6 and 7, respectively.

Table 7. Residual stresses by X-rays diffraction and MBN techniques.

Samples	**Residual Stresses (MPa)**			
	X-ray diffraction	**Average**	**MBN**	**Average**
1	-350	-330	-314	**-296**
2	-310		-336	
3	8	-11.5	69	**16**
4	15		-38	
5	173	224	157	**239**
6	275		270	

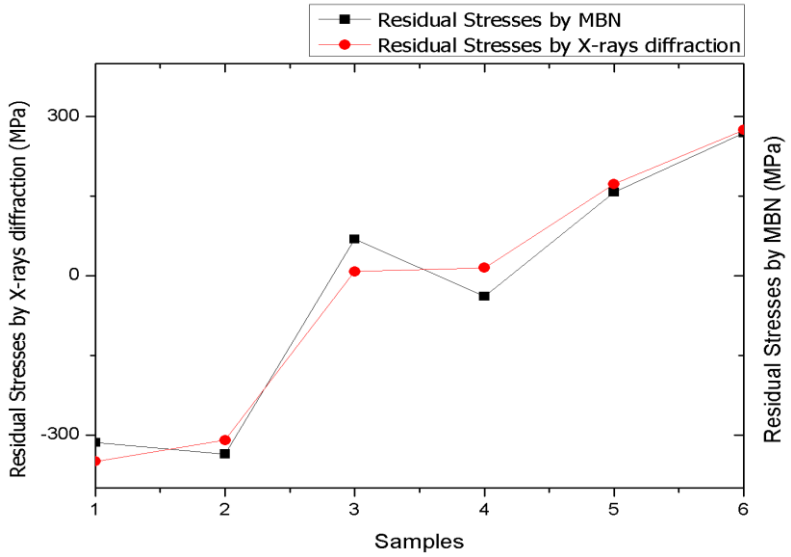

Figure 7. Residual stresses by X-ray diffraction and MBN techniques.

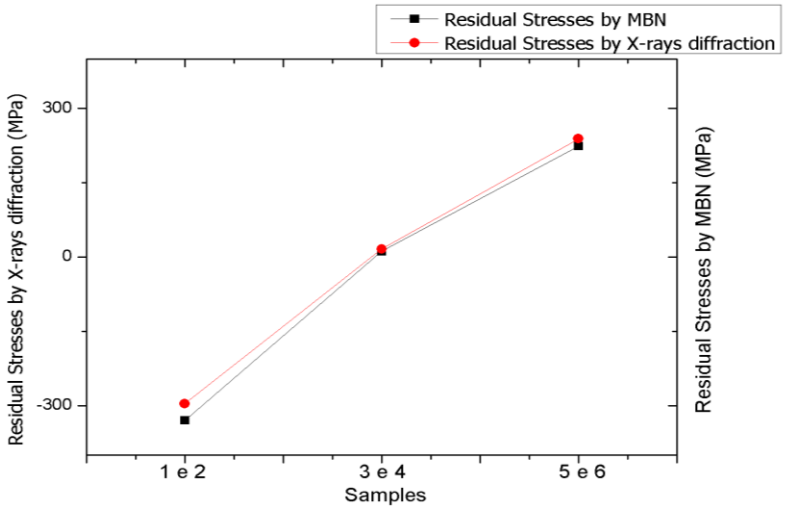

Figure 8. Residual stresses average by X-ray diffraction and MBN techniques.

Figure 8 shows the relationship between the residual stresses and the MBN signal of all the samples. It is reasonable to assume that there was a coherence of the results point-to-point, since all stresses behave in a similar way and describe linearity, a result corroborated by Figure 6, in which all average residual stresses are presented.

Therefore, as shown in Figures 5 and 6, the residual stresses calculated by the MBN had a satisfactory behavior concerning to the results obtained by the well established measurement technique – X-ray diffraction. The correlation between the techniques was more successful since the adjustment coefficient R2 was approximately equal to 0.98, indicating to be close to 1 (ideal), according to Kurushina et al. (2018), demonstrating success in measurement.

4. CONCLUSIONS

This study compared the use of two techniques, X-ray diffraction and Magnetic Barkhausen noise (MBN), for residual stress analysis in P91 steel samples and it can be concluded that:

1. In areas containing residual compressive stresses, magnetic Barkhausen noise values are lower than those with residual tensile stresses.

2. MBN technique allows to qualify residual stresses and presents great potential for field application to characterize residual and applied stresses.

3. The calibration curve makes it possible to effectively correlate the residual stresses by the two measurement methods.

5. ACKNOWLEDGEMENTS

This study was financed in part by the *Coordenação de Aperfeiçoamento de Pessoal de Nível Superior -Brasil (CAPES)* - FinanceCode 001. The authors would also like to thank the Brazilian research agencies CNPq and FAPERJ, for the financial support.

6. REFERENCES

Alves, M. C. S.; Bianchi, E. C.; Aguiar, P. R.; Catai, R. E. "Variable feed-rate influence on the final quality of metal grinding". *Revista Escola de Minas*, Vol. 62, p. 65-71, 2009.

Choudhary, B. K., Christopher, J., 2019. "Influence of temperature and strain rate on tensile deformation and fracture behavior of boron added P91 steel*". International Journal of Pressure Vessels and Piping*, Vol. 171, pp. 153-161.

Cindra Fonseca, M.P., 2000. *EVolução do estado de tensões residuais em juntas soldadas de tubulação durante ciclos de fadiga*. Ph.D. thesis, Universidade Federal do Rio de Janeiro - COPPE/UFRJ, Rio de Janeiro, Brasil.

Groover, M. P., 2014. *Fundamentals os Modern Manufacturing: Materials, Processes and Systems*. John Wiley& Sons, 4nd Edition.

Kurushina, VOL, Pavlovskaia, E., Postnikov, A., Wiercigroch, M., "Calibration and comparison of VIV wake oscillator models for low mass ratio structures", *International Journal of Mechanical Sciences*, Vol. 142, 2018, pp. 547-560.

Li, H. Y., Sun, H.L., Bowen, P., and Knott, J. F., 2018. "Effects of compressive residual stress on short fatigue crack growth in a nickel-based superalloy". *International Journal of Fatigue*, Vol. 108, pp. 53-61.

Pandey, C., Mahapatra, M., Kumar, P., Saini, N., 2018. "Some studies on P91 steel and their weldments". *Journal of Alloys and Compounds*, Vol. 743, pp. 332-364.

Qimeng, Z., Jia, C., Guoqing, G., Hui, C., and Peng, L., 2017. "Ameliorated longitudinal critically refracted – Attenuation velocity method for welding residual stress measurement". *Journal of Material Processing Technology*, Vol. 205, pp. 267-275.

Sorsa, A., Santa-aho, S., Wartlaunen, J., Suominem, L., Vippola, M. and Leiviska, K., 2018. "Effects of Shot Peening Parameters to Residual Stress Profiles and Barkhausen Noise". *Journal of Nondestructive Evaluation*, Vol. 37, pp.53-61.

Wang, Y.; Gil, P.R.; Chen, Y.H.; Kromrey, J.; Kim, E.S.; Pham, T.; Nguyen, D.; Romano, J.L. "Comparing the Performance of Approaches for Testing the Homogeneity of Variance Assumption in One-Factor ANOVA Models", *Educational and Psychological Measurement*, Vol. 77, n. 2, pp. 305-329, 2017.

Zhou, N.; Peng, R. L.; Pettersson, R. "Surface integrity of 2304 duplex stainless steel after different grinding operations", *Journal of Materials Processing Tech.*, Vol. 229, 2016, pp.294-30.

Zoei, S. M.; Sadeghi, M. H.; Salehi, M. "Effect of grinding parameters on the wear resistance and residual stress of HVOF-deposited WC–10Co–4Cr coating", *Surface & Coatings Technology*, Vol. 307, p. 886-891, 2016.

7. RESPONSIBILITY NOTICE

The authors are the only responsible for the printed material included in this paper.